

Anionic and Neutral 2D indium metal-organic frameworks as catalysts for the Ugi one-pot multicomponent reaction

Daniel Reinares-Fisac, Lina M- Aguirre-Díaz, Marta Iglesias, Enrique Gutiérrez-Puebla, Felipe Gándara, M. Ángeles Monge

Supporting material

S1. Experimental procedure	S-2
• General	
• Catalytic activity experiments procedure	
S2. Single crystal x-ray diffraction and structure of InPF-50 and InPF-51	S-3
S3. Characterization of InPF-50	S-5
S4. Characterization of InPF-51	S-7
S5. Catalytic activity experiments background	S-10
S6. Catalytic activity data	S-11
S7. Recycle and scaled reactions	S-13
S8. Characterization of the Ugi-4C reaction products	S-15
S9. References	S-19

- **S1. EXPERIMENTAL PROCEDURE**

1.1. General

All reagents and solvents employed were commercially available and used as received without further purification: $\text{In}(\text{NO}_3)_3 \cdot x\text{H}_2\text{O}$ (99.999%-In PURATREM from Strem Chemicals); $\text{InCl}_3 \cdot 4\text{H}_2\text{O}$ (purchased from Alfa Aesar); 1,3,5-tris(4-carboxyphenyl)benzene [H_3btb] (purchased from Strem Chemicals); N,N-dimethylformamide (DMF; from Sharlab) and nitric acid 69.5% reagent grade (from Sharlab). Powder X-ray diffraction (PXRD) patterns were measured with a Bruker D8 diffractometer with a copper source operated at 1600 W, with step size = 0.02° and exposure time = 0.5 s/step. PXRD measurements were used to check the purity of the obtained microcrystalline products by a comparison of the experimental results with the simulated patterns obtained from single-crystal X-ray diffraction data. IR spectra were recorded from KBr pellets in the range $4000\text{--}400\text{ cm}^{-1}$ on a Nicolet FT-IR 20SXC spectrometer. Thermogravimetric and differential thermal analysis (TGA-DTA) was performed using a SDT Q600 from TA Instruments equipment in a temperature range between 30 and 800°C in air (100 mL/min flow) atmosphere and heating rate of $10^\circ\text{C}/\text{min}$. A CNHS PERKIN ELMER 2400 analyzer was employed for the elemental analysis. NMR spectra were recorded in a Bruker AMX-300 equipment using CDCl_3 as solvent. Exact mass measurements were performed in an ABSciex QSTAR equipment employing “Electrospray ionization” (ESI) method.

1.5. Catalytic activity experiments procedure

Catalyst was activated by heating at 150°C for a period of 24 hours after being soaking in ethanol. The mixture of aldehyde, amine, benzoic acid and cyclohexyl isocyanide was added into a Schlenk tube (0.76 mmol of aldehyde, 0.76 mmol of amine, 0.84 mmol of benzoic acid and 0.76 mmol of cyclohexyl isocyanide), where the MOF and the ethanol as solvent (up to 1 mL) have been previously introduced (10 mg for 1 mol%). The 10% of excess of benzoic acid in relation to the other substrates is used as a pattern in ^1H NMR. The mixture was stirred (600 rpm) at 25°C , under N_2 -atmosphere. Before making the NMR measurement, the sample was dried in order to reduce the amount of ethanol, and after dissolved in CDCl_3 . For comparative purpose, the same standard reaction conditions were used for all tested substrates, and therefore the reaction parameters were not further optimized for each one of them. When reactions were completed the content of the Schlenk tube was mixed with DCM in order to dissolve the compounds and recover the catalyst by filtration. X-ray diffraction patterns were obtained for each experiment to ensure crystallinity, purity and recyclability of the MOF. A blank test without catalyst was performed within the conditions previously described. A leaching test was performed followed by an ICP-MS analysis which showed that no indium metal was dissolved. A chromatographic column separation was also performed to confirm the reported yield isolating the obtained product. For this procedure, a column of 8 cm high and 2 cm of diameter was made and a 6:1 ratio of heptane/ethyl acetate relation has been used.

Catalyst InPF-51 was reused in 10 cycles. In each case, after recovery, the MOF was washed with DCM and ethanol, then dried overnight following the same procedure described above.

- **S2. X-RAY STRUCTURE DETERMINATION**

2.1 Main crystallographic data for InPF-50 and InPF-51

Table S1 summarizes the main crystal and refinement data for **InPF-51**. Crystals were selected under a polarizing optical microscope for a single-crystal X-ray diffraction experiment. Single-crystal X-ray data were obtained in a Bruker four circle kappa-diffractometer equipped with a Cu INCOATED microsource, operated at 30 W power (45kV, 0.60mA) to generate Cu K α radiation ($\lambda = 1.54178 \text{ \AA}$), and a Bruker VANTEC 500 area detector (microgap technology). Diffraction data were collected exploring over a hemisphere of the reciprocal space in a combination of φ and ω scans to reach a resolution of 0.85 \AA , using a Bruker APEX3² software suite (each exposure, depending on ω , was between 20 and 100 s covering 1 $^\circ$ in ω or φ). Unit cell dimensions were determined for least-squares fit of reflections with $I > 2.5\sigma$. The structures were solved by intrinsic phase methods.³ The hydrogen atoms were fixed at their calculated positions using distances and angle constraints. All calculations were performed using APEX3 software for data collection and OLEX2-1.2⁴ and SHELXTL⁵ to resolve and refine the structure.

Table S2.1 Main crystallographic data for InPF-50 (CCDC number 1483221).

Identification code	InPF50
Empirical formula	C ₃₀ H ₁₈ InNO _{10.5}
Formula weight	675.27
Temperature/K	250
Crystal system	orthorhombic
Space group	Pbcn
a/\AA	17.5574(8)
b/\AA	20.8944(9)
c/\AA	16.8168(8)
α/$^\circ$	90
β/$^\circ$	90
γ/$^\circ$	90
Volume/\AA^3	6169.3(5)
Z	8
ρ_{calc}/g/cm³	1.454
μ/mm⁻¹	6.623
F(000)	2704.0
Crystal size/mm³	0.175 \times 0.175 \times 0.075
Radiation	CuK α ($\lambda = 1.54178$)
2θ range for data collection/$^\circ$	6.576 to 130.532
Index ranges	-20 \leq h \leq 20, -24 \leq k \leq 23, -19 \leq l \leq 19
Reflections collected	30660
Independent reflections	5195 [$R_{\text{int}} = 0.0600$, $R_{\text{sigma}} = 0.0389$]
Data/restraints/parameters	5195/0/378
Goodness-of-fit on F²	1.158
Final R indexes [$I \geq 2\sigma(I)$]	$R_1 = 0.0866$, $wR_2 = 0.2445$
Final R indexes [all data]	$R_1 = 0.1008$, $wR_2 = 0.2618$
Largest diff. peak/hole / e \AA^{-3}	1.17/-1.23

Table S2.2 Main crystallographic data for InPF-51 (CCDC number 1873905).

Identification code	InPF51
Empirical formula	C ₆₁ H ₅₂ Cl ₂ In ₂ N ₃ O ₁₃
Formula weight	1335.62
Temperature/K	150
Crystal system	monoclinic
Space group	P2 ₁ /n
a/Å	17.3589(6)
b/Å	13.0410(6)
c/Å	25.9082(9)
α/°	90
β/°	91.109(2)
γ/°	90
Volume/Å³	5863.9(4)
Z	4
ρ_{calc}/cm³	1.505
μ/mm⁻¹	7.587
F(000)	2686.0
Crystal size/mm³	0.2 × 0.15 × 0.08
Radiation	CuKα (λ = 1.54178)
2θ range for data collection/°	6.074 to 132.596
Index ranges	-20 ≤ h ≤ 20, -15 ≤ k ≤ 15, -30 ≤ l ≤ 30
Reflections collected	55360
Independent reflections	10104 [R _{int} = 0.0709, R _{sigma} = 0.0493]
Data/restraints/parameters	10104/0/746
Goodness-of-fit on F²	1.030
Final R indexes [I>=2σ (I)]	R ₁ = 0.0671, wR ₂ = 0.1833
Final R indexes [all data]	R ₁ = 0.0798, wR ₂ = 0.1953
Largest diff. peak/hole / e Å⁻³	2.82/-1.18

- **S3. CHARACTERIZATION OF InPF-50**

Formula $[\text{In}(\text{btb})(\text{DMF})(\text{H}_2\text{O})]\cdot\text{L}$, InPF-50 CCDC number 1483221.

3.1 X-ray diffraction pattern (PXRD)

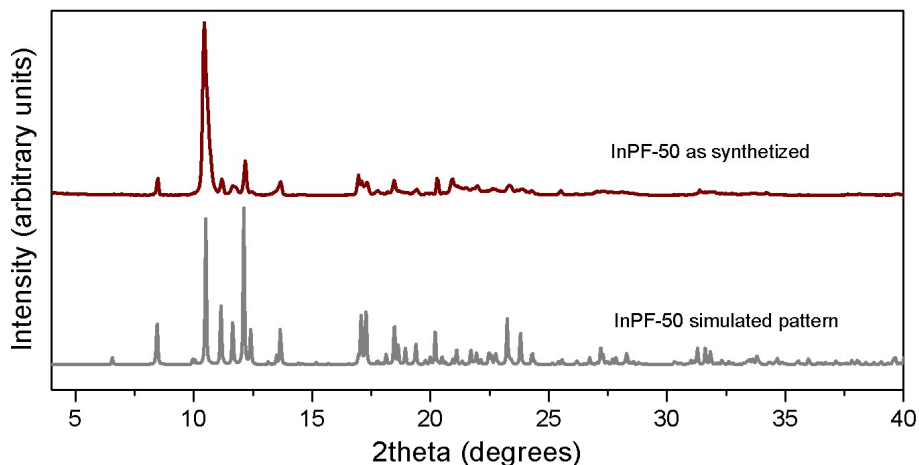


Figure S3.1 Simulated profile from single-crystal diffraction structure data of InPF-50 (gray) and experimental profile from powder x-ray diffraction (red). The experimental spectrum is affected by the layered structure of crystals.

3.2 IR spectra (KBr; cm^{-1})

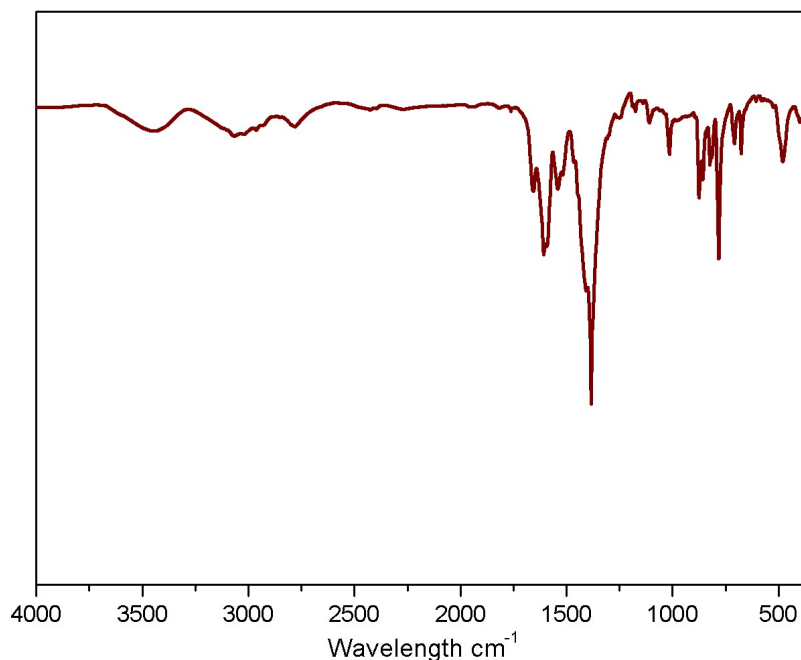


Figure S3.2 Infrared transmittance spectra, in the 4000-400 cm^{-1} range, of MOF InPF-50. IR (KBr, cm^{-1}): 3480 ν (O-H), 3059 ν (aromatic C-H), 2781 ν (C-H), 1661, 1599, 1588 ν (C=O), 1547 and 1517 ν (C=C), 1404 ν (C-C), 1166, 1098, 1020, 879, 848, 818 ν (aromatic C-C), 787 and 708 ν (C-C), 469 ν (In-O).

3.3 Thermogravimetric analysis (TGA)

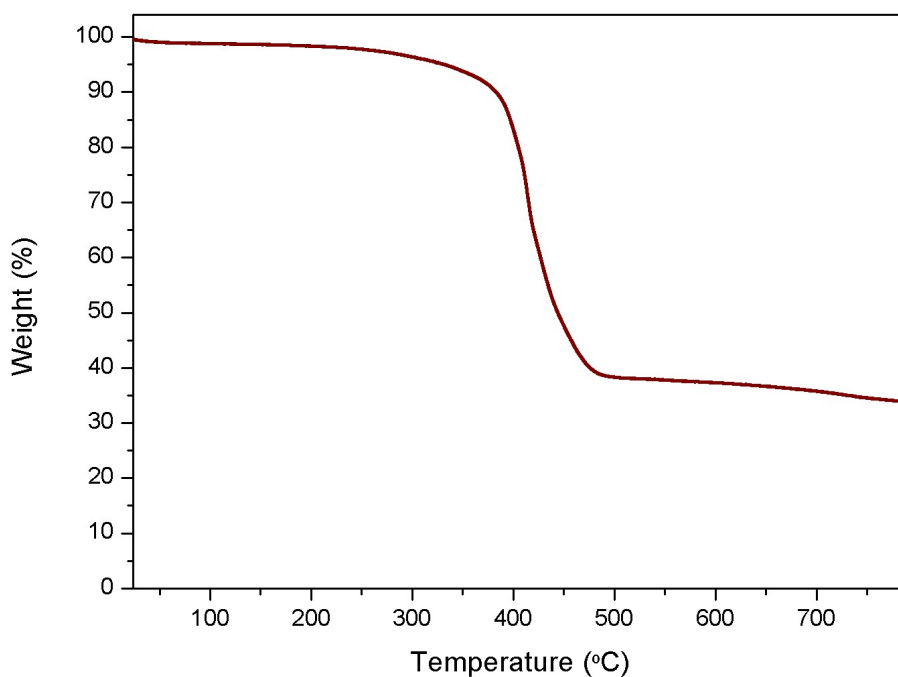


Figure S3.3.a TG analysis performed in N_2 , between 30 and 800°C (100 mL/min flow) and a heating rate of 10°C per minute. A first loss of 2% occurs until 150°C, when the H_2O molecule goes away. After 150, until the structure collapses at 400°C, another loss of 9% is related with the DMF molecule. After 450°C, amorphous carbon matrix remains.

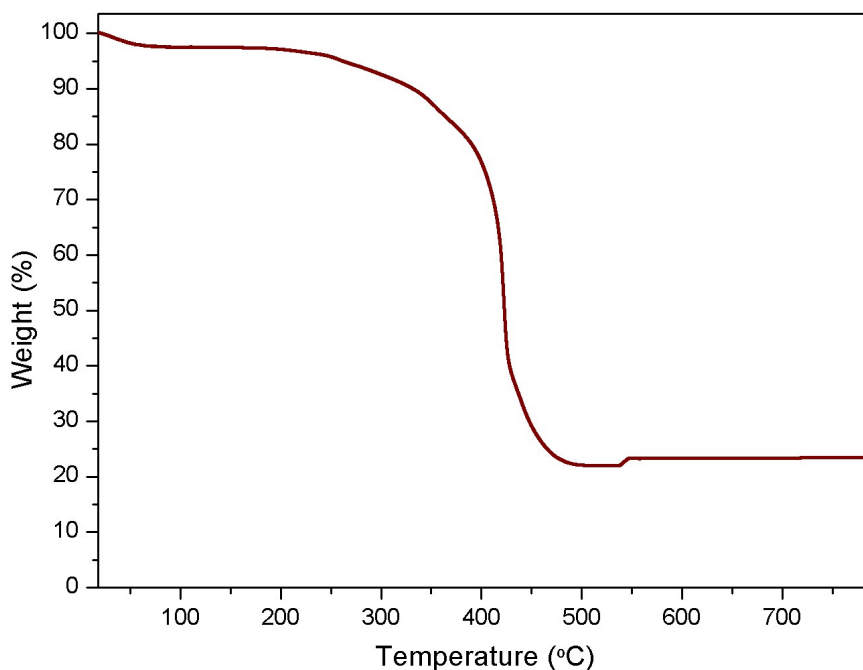


Figure S3.3.b TG analysis performed in air, between 30 and 800°C (100 mL/min flow) and a heating rate of 10°C per minute. A first loss of 2.7% occurs until 150°C, and it is related solvent (water and ethanol) and to the coordinated H_2O molecule. After 150, until the structure collapses at 320°C, another loss of 9% fits with the leak of the DMF molecule. After 450°C only indium oxide can be found.

• **S4. CHARACTERIZATION OF InPF-51**

Formula $[\text{In}_2(\text{btb})_2(\text{Cl})_2] \cdot [(\text{CH}_3)_2\text{NH}_2^+]_2 \cdot \text{L}$, InPF-51 CCDC number 1873905.

4.1 X-ray diffraction pattern (PXRD)

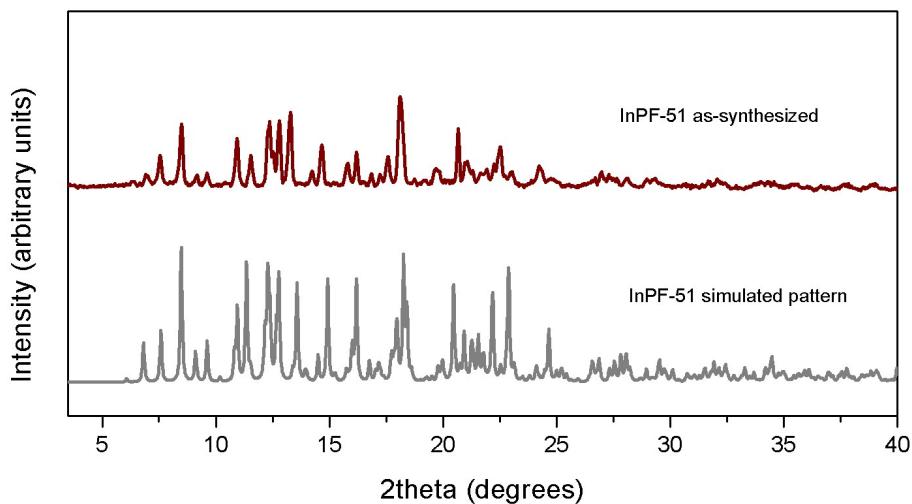


Figure S4.1 Simulated profile from single-crystal diffraction structure data of InPF-51 (gray) and experimental profile from powder x-ray diffraction (red).

4.2 IR spectra (KBr; cm^{-1})

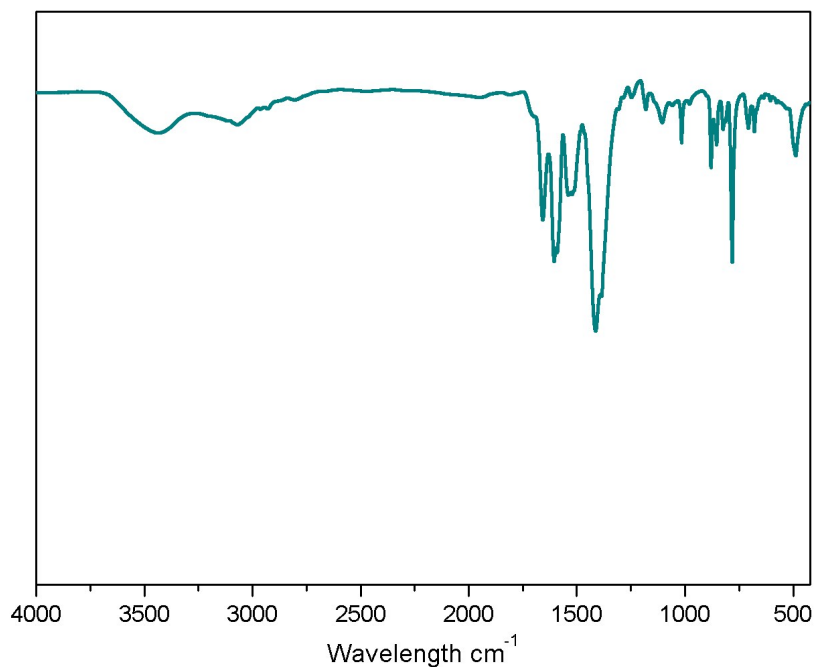


Figure S4.2 Infrared transmittance spectra, in the 4000-400 cm^{-1} range, of MOF InPF-51. IR (KBr, cm^{-1}): 3445 ν (O-H), 3062 ν (aromatic C-H), 1649, 1598 and 1587 ν (C=O), 1521 and 1380 ν (aromatic C-C), 1245 ν (C-O), 1410 ν (C-C), 1175, 1104, 1024, 883, 852, 832 and 711 ν (C-C) aromatic, 782 and 671 ν (C-C), 489 ν (In-O).

4.3 Thermogravimetric analysis (TGA)

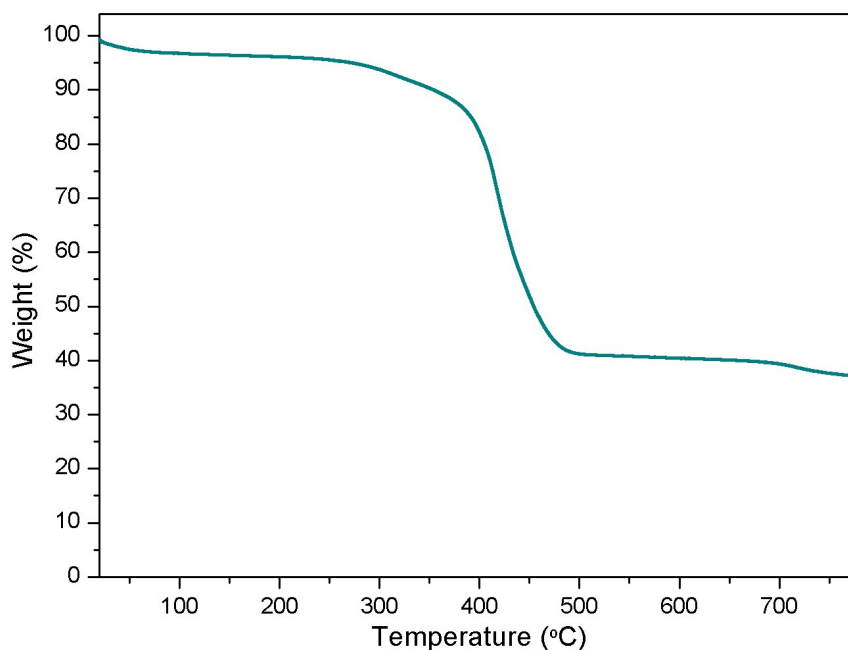


Figure S4.3.a Thermogravimetric thermal analyses (TG-DTA) were performed in a temperature range between 30 and 800 °C in N₂ (100 mL/min flow) and a heating rate of 10°C per minute. The first loss of mass, 3.2%, expressed in the first slight slope until 150°C, corresponds to solvent, mainly water and ethanol. Then, coordinated water, dimethylamine and DMF subproducts evacuate from 150 to 330°C, which corresponds to a loss of 4.5% of the total weight. The structure finally collapses when temperature reaches 400°C. Amorphous carbon matrix remains.

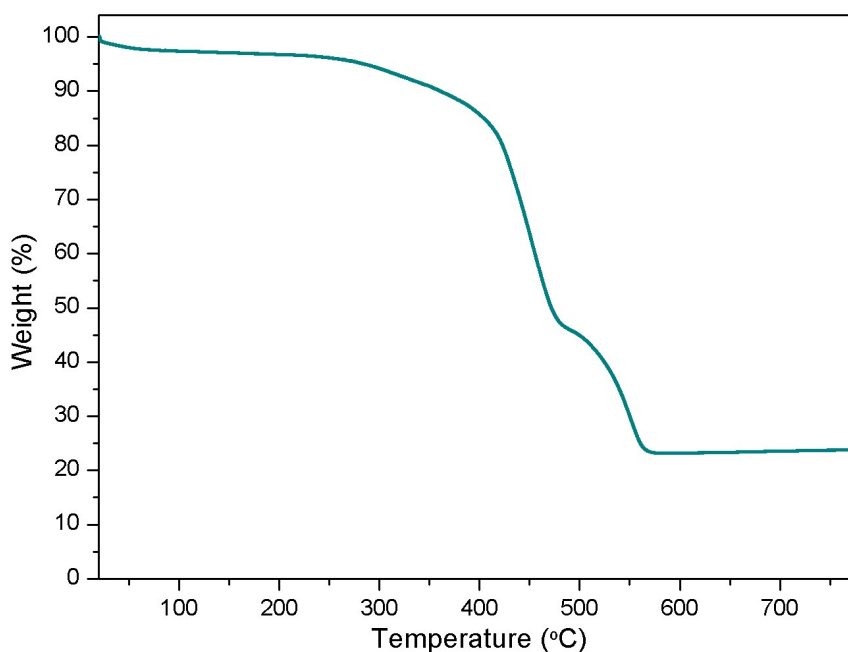


Figure S4.3.b TG analysis performed in air, between 30 and 800°C (10 mL/min flow) and a heating rate of 10°C per minute. The losses of mass are like those that occur in nitrogenous atmosphere. Structure collapses at 400°C. Between 450 and 550, organic part is lost. Only Indium oxide remains as a yellowish product.

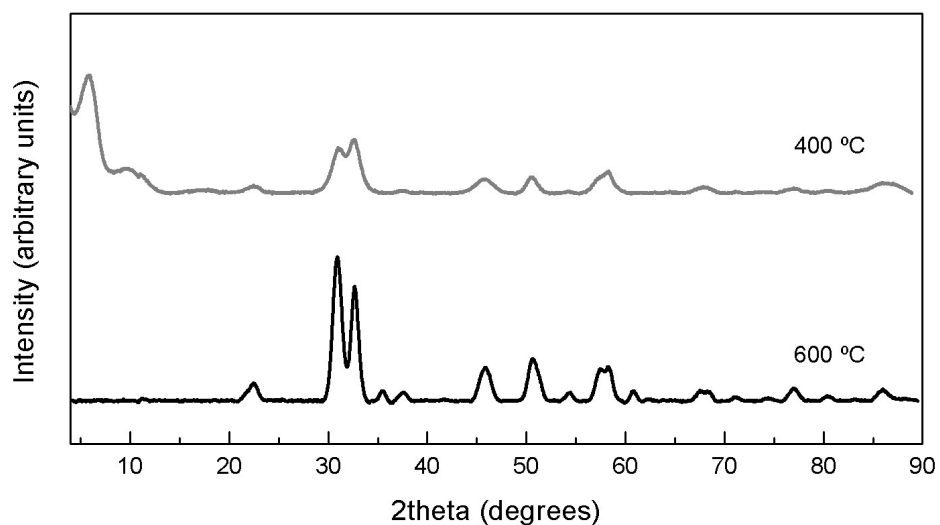


Figure S3.3.c Powder X-ray diffraction of residues after thermogravimetric analysis in nitrogen atmosphere. At 400°C the presence of oxide is observed, together with InPF-51 that remains. Later, at 600°C only crystalline In_2O_3 is detected by XRD.

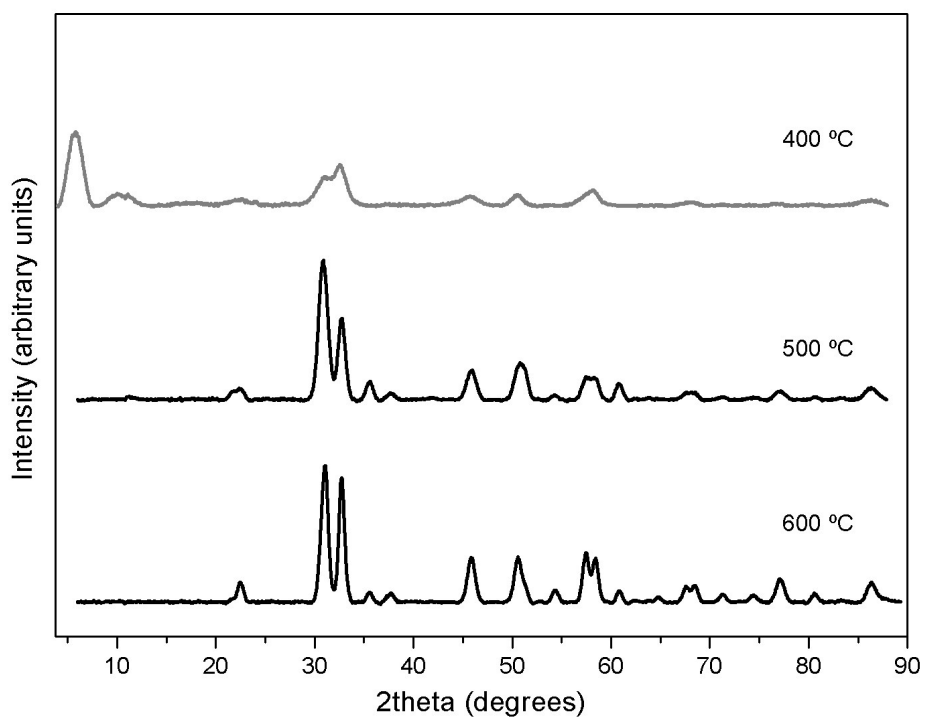
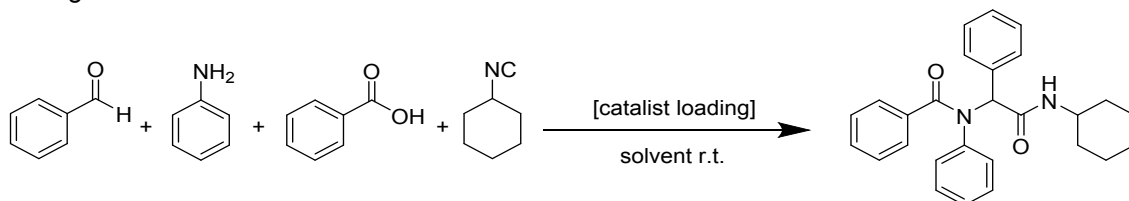


Figure S3.3.d Powder X-ray diffraction of residues after thermogravimetric analysis in air atmosphere. At 400°C oxide and MOF is observed. At 500°C only In_2O_3 is detected, which is more crystalline at 600°C. No organic matter is observed.

• **S5. CATALYTIC ACTIVITY EXPERIMENTS BACKGROUND**

Table S5.1 Catalytic activity of several homogeneous and heterogeneous catalysts used in the 4C-Ugi reaction



Catalyst	Type	Reaction conditions	Time and yield	Reference
	homogenous	Polyethylene glycol-water, r.t.	30 min; 77-91 %	Niu <i>et al.</i> ⁶
butyl-3-methyl-imidazolium tetrafluoroborate [(bmim)BF ₄]	homogeneous	ionic liquid, r.t.	8 h; 74 %	Singh <i>et al.</i> ⁷
-	homogeneous	Urea-choline chloride, ionic liquid, r.t.	3 h; 90 %	Azizi <i>et al.</i> ⁸
-	homogeneous	Methanol, r.t.	3 h; 40 %	Azizi <i>et al.</i> ⁸
-	homogeneous	Water, r.t.	3 h; 45 %	Azizi <i>et al.</i> ⁸
-	homogeneous	CH ₂ Cl ₂ , r.t.	3 h; 30 %	Azizi <i>et al.</i> ⁸
-	homogeneous	CH ₃ CN, r.t.	3 h; 45 %	Azizi <i>et al.</i> ⁸
InCl ₃ ·4H ₂ O	homogeneous	1 mol%, ethanol, r.t.	1h; 9 %	this work*
In(NO ₃) ₃ ·xH ₂ O	homogeneous	1 mol%, ethanol, r.t.	1h; 5 %	this work*

*Final product analyzed by ¹H NMR.

Table S5.2 Catalytic activity of different *p*-MOFs in the one-pot 4C-Ugi reaction.

Catalyst	Type	Reaction conditions	Time and yield	Reference
InPF-16	heterogeneous	1 mol%, r.t., EtOH	2 h; traces	Monge <i>et al.</i> ⁹
InPF-17	heterogeneous	1 mol%, r.t., EtOH	2 h; 92 %	Monge <i>et al.</i> ⁹
InPF-18	heterogeneous	1 mol%, r.t., EtOH	2 h; 67 %	Monge <i>et al.</i> ⁹
InPF-20	heterogeneous	1 mol%, r.t., EtOH	2 h; 89 %	Monge <i>et al.</i> ⁹

- **S6. CATALYTIC ACTIVITY DATA**

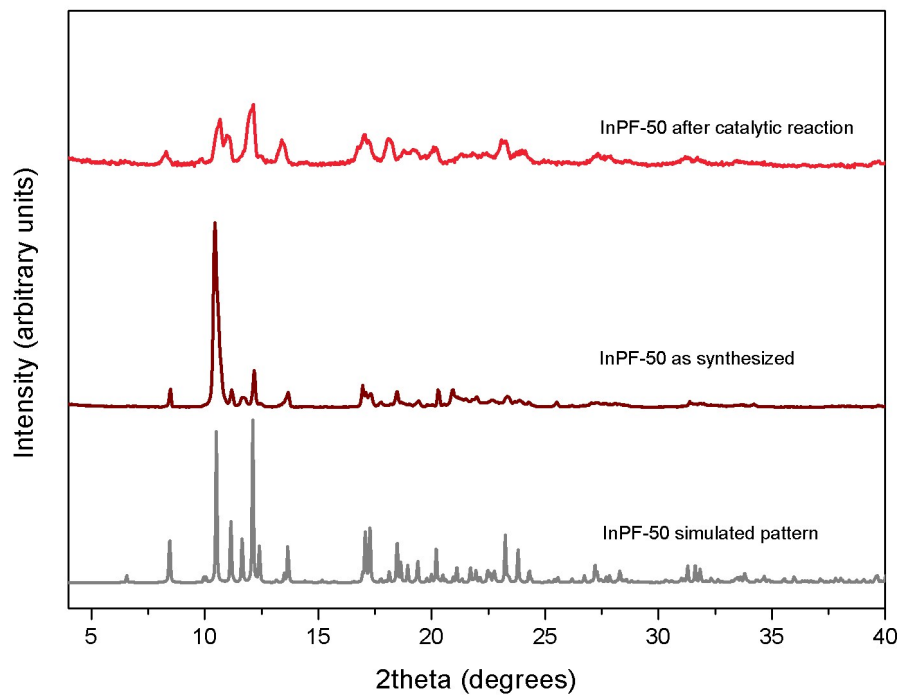


Figure S6.1.a InPF-50 simulated pattern (gray), as-synthesized and after standard catalytic reaction.

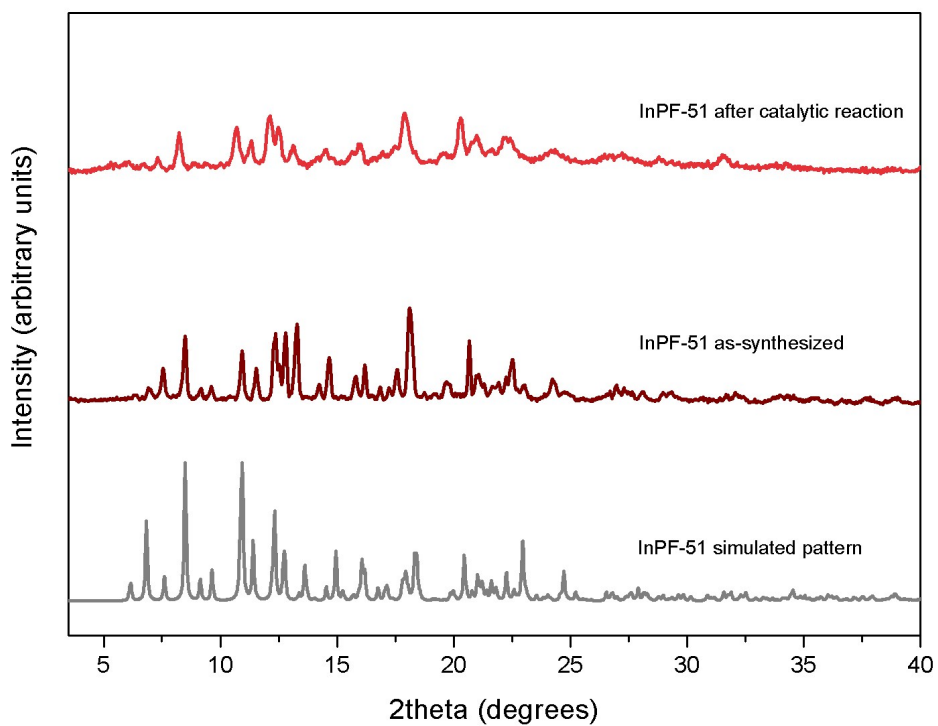


Figure S6.1.b InPF-51 simulated pattern (gray), as-synthesized and after standard catalytic reaction.

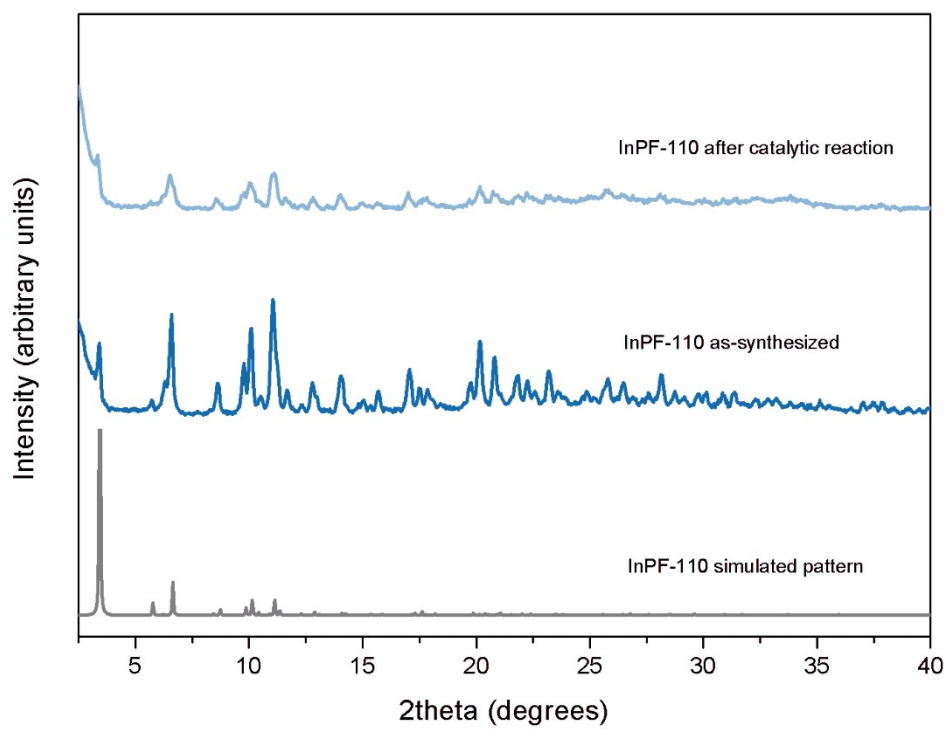


Figure S6.1.c InPF-110 simulated pattern (gray), as-synthesized and after standard catalytic reaction.

• **S7. RECYCLE AND SCALED REACTIONS**

Table S7 Ugi one-pot four component reaction using benzaldehyde, benzoic acid, cyclohexyl isocyanide (1.1:1:1.1:1) up to 10 cycles, using InPF-51 as catalyst.

Entry	Yield ^a (%)	TON ^b
Cycle 1	90 %	90
Cycle 2	90 %	90
Cycle 3	90 %	90
Cycle 4	90 %	90
Cycle 5	90 %	90
Cycle 6	90 %	90
Cycle 7	90 %	90
Cycle 8	88 %	88
Cycle 9	87 %	87
Cycle 10	83 %	83
Scale x5	90 %	90

^aYield by ¹H NMR.

^bTON = (mmol substrate/ mmol catalyst).

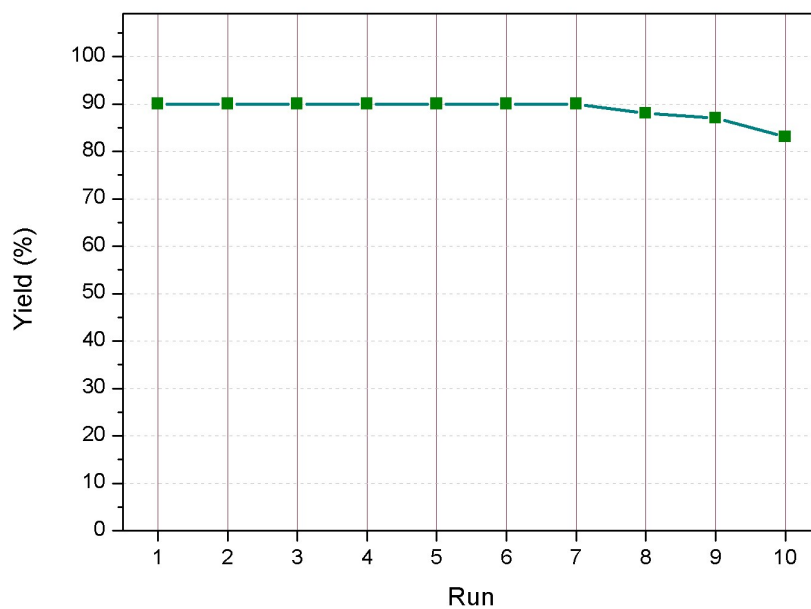


Figure S7.1 Graph with recycle run yields obtained, from the first to the tenth.

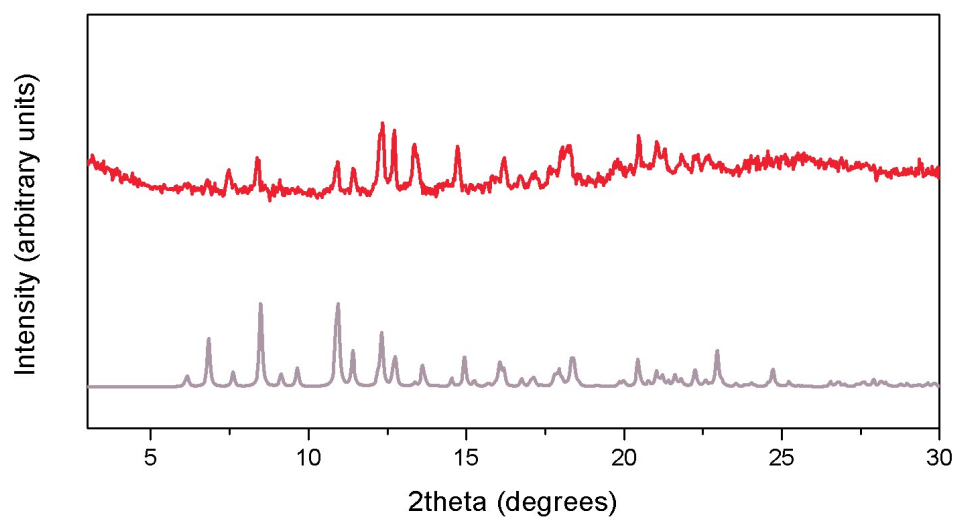
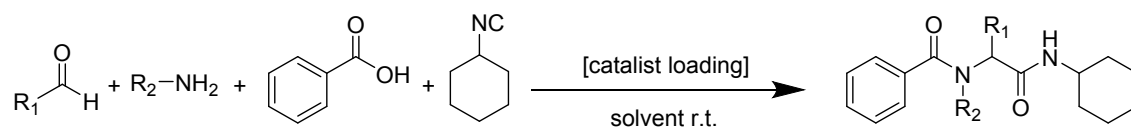
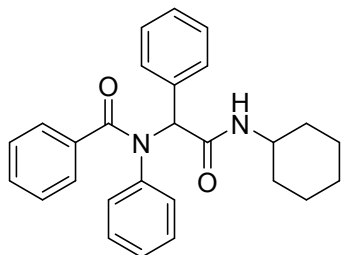


Figure S7.2 Simulated profile from InPF-51 single-crystal diffraction structure data (grey) and after the tenth run in catalytic activity experiments (red).

• **S8. CHARACTERIZATION OF THE UGI 4C REACTION PRODUCTS**



8.1 Ugi-4CR product: N-((cyclohexylaminocarbonyl)(phenyl)methyl)-N-phenylbenzamide



White solid: H^+ NMR (300 MHz, $CDCl_3$): $\delta = 1.07\text{-}1.95$ (m, 10H, from $-CH_2$; cyclohexyl), 3.88 (m, 1H, from $-CH$; cyclohexyl), 5.83 (broad singlet, 1H, from $-NH$), 6.17 (s, 1H, from $-CH$ aliphatic), 7.01-7.35 (m, 15H, from $-CH$ aromatic). IR (KBr) ν (cm^{-1}): 3257, 3074, 2933, 2852, 1645, 1592, 1555, 1502, 1451, 1391, 1340, 1251, 1182, 1142, 1103, 1073, 1033, 1002, 972, 922, 885, 805, 753, 727, 703, 653, 563, 513. (This corresponds with the spectrum reported for compound with CAS No. 1266385-49-2) Elemental analysis [found (calculated)] C: 77.54% (78.60); H: 7.03% (6.84); N: 6.50% (6.79). ESMS: m/z : $[M+H]^+$: 413; $[M+Na]^+$: 435. This compound is known.⁷

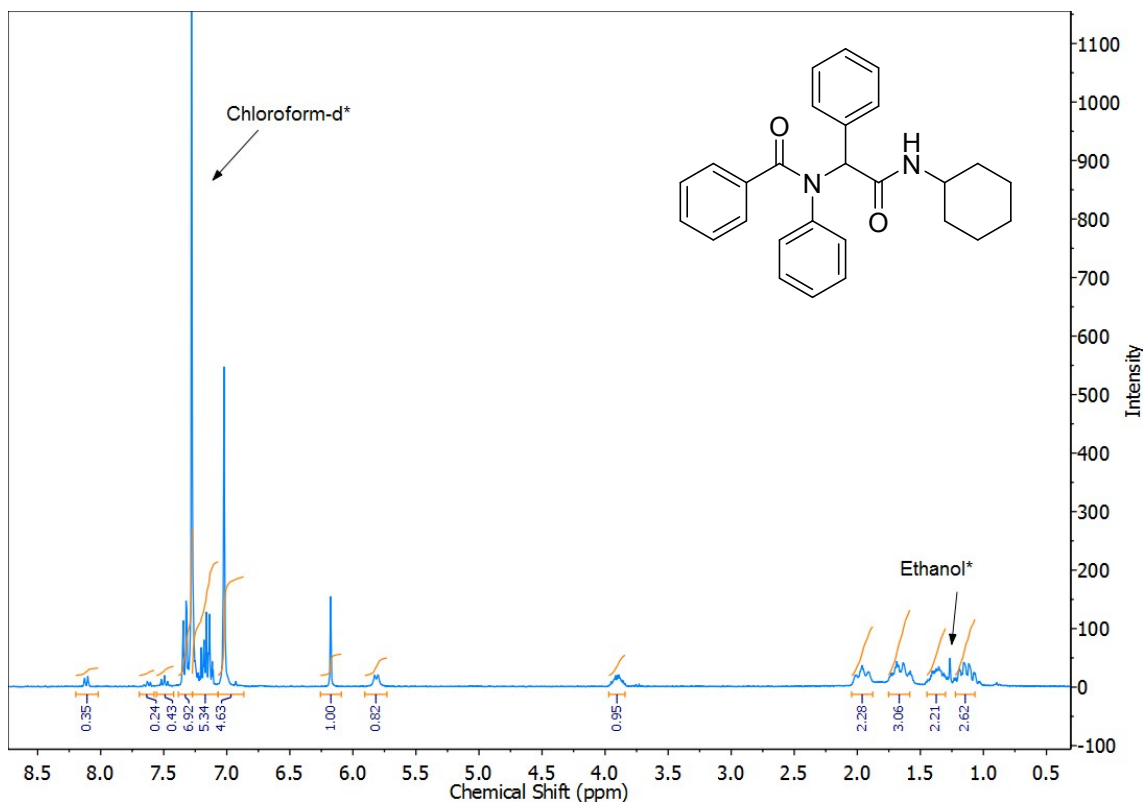


Figure S8.1.a ^1H NMR spectra of **N-((cyclohexylaminocarbonyl)(phenyl)methyl)-N-phenylbenzamide**. Peaks from 7.47 to 8.15 belong to benzoic acid, added a 10% in excess to quantify the amount of final product.

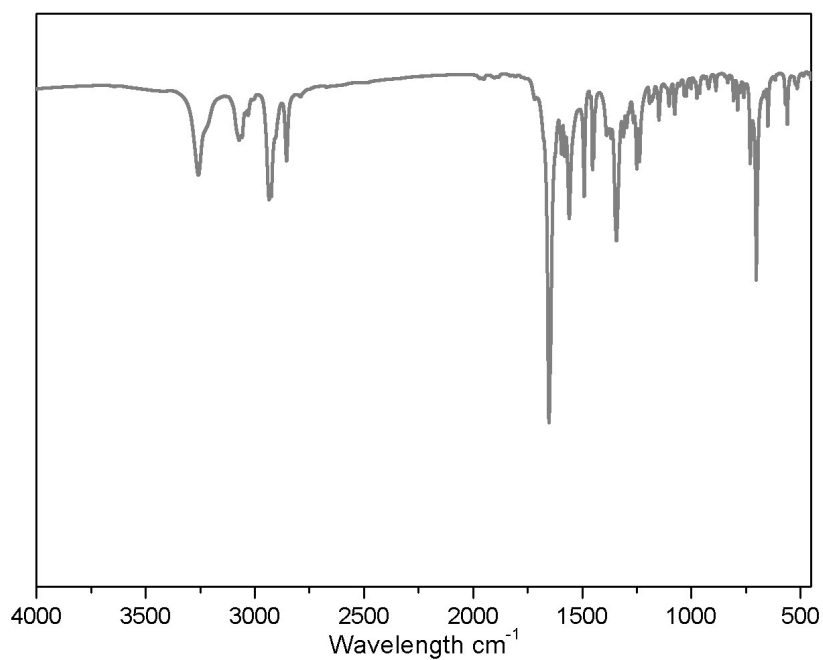


Figure S8.1.b Infrared spectra for N-((cyclohexylaminocarbonyl)(phenyl)methyl)-N-phenylbenzamide, in the 4000-400 cm^{-1} range.

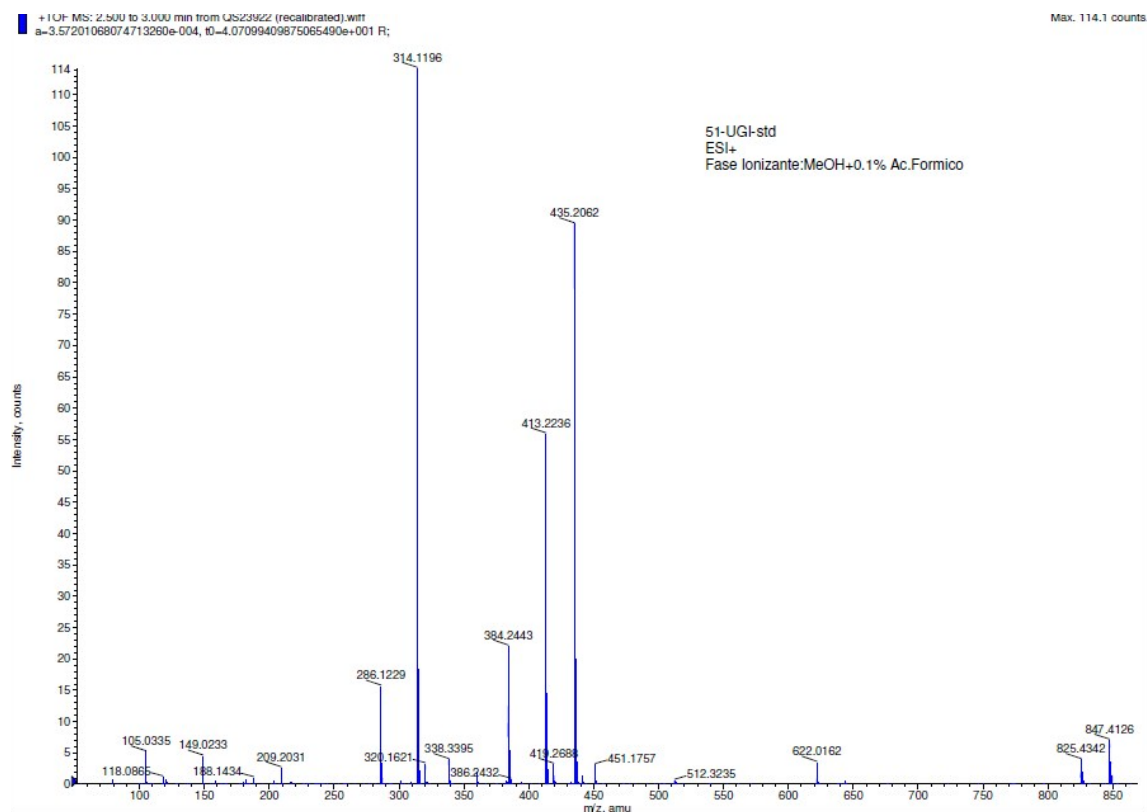
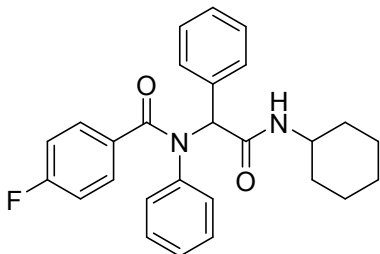


Figure S8.1.c ESI-MS spectra for N-((cyclohexylaminocarbonyl)(phenyl)methyl)-N-phenylbenzamide.

8.2 Ugi-4CR products characterization

- Benzeneacetamide, α -[(4-fluorophenyl)(4-methylbenzoyl)amino]-N-cyclohexyl-

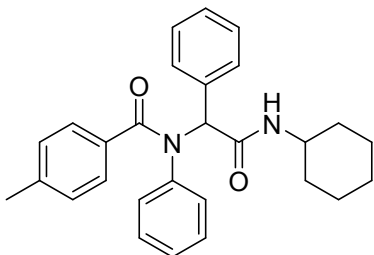
Table S6.2 ENTRY 2



White solid: H^+ NMR (300 MHz, $CDCl_3$): δ = 1.11-2.03 (m, 10H, from $-CH_2$; cyclohexyl), 3.91 (m, 1H, from $-CH$; cyclohexyl), 5.87 (d, 1H, from $-NH$), 6.20 (s, 1H, from $-CH$ aliphatic), 6.92-7.34 (m, 14H, from $-CH$ aromatic).

- Benzeneacetamide, α -[(4methylphenyl)(4-methylbenzoyl)amino]-N-cyclohexyl-

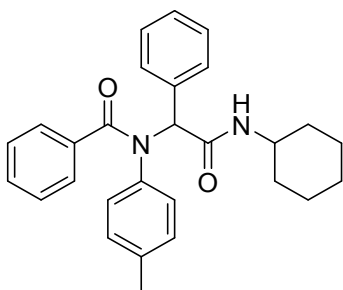
Table S6.2 ENTRY 3



White solid: H^+ NMR (300 MHz, $CDCl_3$): δ = 1.03-1.96 (m, 10H, from $-CH_2$; cyclohexyl), 2.29 (s, 3H, from $-CH_3$), 3.85 (m, 1H, from $-CH$; cyclohexyl), 5.72 (d, 1H, from $-NH$), 6.09 (s, 1H, from $-CH$ aliphatic), 7.01-7.32 (m, 15H, from $-CH$ aromatic).

- Benzeneacetamide, α -[benzoyl(4-methylphenyl)amino]-N-cyclohexyl-

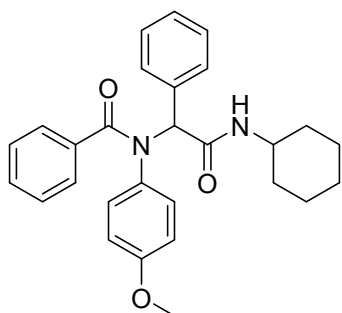
Table S6.2 ENTRY 4



Whitish solid: H^+ NMR (300 MHz, $CDCl_3$): δ = 1.06-2.00 (m, 10H, from $-CH_2$; cyclohexyl), 2.19 (s, 3H, from $-CH_3$) 3.90 (m, 1H, from $-CH$; cyclohexyl), 5.86 (d, 1H, from $-NH$), 6.15 (s, 1H, from $-CH$ aliphatic), 6.81-7.37 (m, 14H, from $-CH$ aromatic).

- α -[benzoyl(4-methoxyphenyl)amino]-N-cyclohexyl- benzeneacetamide

TABLE S6.2 ENTRY 5



Grayish solid: H^+ NMR (300 MHz, $CDCl_3$): δ = 1.04-1.98 (m, 10H, from $-CH_2-$; cyclohexyl), 3.67 (s, 3H, from $-CH_3$) 3.87 (m, 1H, from $-CH$; cyclohexyl), 5.81 (d, 1H, from $-NH$), 6.21 (s, 1H, from $-CH$ aliphatic), 6.50-7.32 (m, 14H, from $-CH$ aromatic).

• **S9. REFERENCES**

- (1) Reinares-Fisac, D.; Aguirre-Díaz, L. M.; Iglesias, M.; Snejko, N.; Gutiérrez-Puebla, E.; Monge M. A.; Gándara, F.; *Journal of the American Chemical Society*, **2016**, 138 (29), 9089-9092
- (2) APEX3: Brucker-AXS: Madison, WI, **2016**
- (3) Sheldrick, G. M. SHELXT-2014, **2013**
- (4) Dolomanov, O. V.; Bourhis, L. J.; Gildea, R. J.; Howard, J. A. K.; Puschmann, H. *J. Appl. Crystallogr.* **2009**, 42, 339-341.
- (5) Sheldrick, G. M. *Acta Crystallogr. Sect. A* **2008**, 64, 112-122
- (6) Niu, T.; Lu, G.; Cai, C.; *Journal of Chemical Research*, **2011**, 35 (8), 444-447
- (7) Kaur, S.; Singh, V.; Kumar, G.; Singh, J.; *Arkivoc*, **2011**, 2011 (2)
- (8) Azizi, N.; Dezfooli, S.; Hashemi, M. M.; *Comptes Rendus Chimie*, **2013**, 16, (12), 1098-1102
- (9) Aguirre-Díaz, L. M.; Iglesias, M.; Snejko, N.; Gutiérrez-Puebla, E.; Monge, M.; *Chemistry - A European Journal*, **2016**, 22 (19), 6654-6665